Article

Reconfigurable Intelligent Surface-Assisted Millimeter Wave Networks: Cell Association and Coverage Analysis

Donglai Zhao , Gang Wang, Jinlong Wang * and Zhiquan Zhou

Communication Research Center, Harbin Institute of Technology, Harbin 150001, China;
17b905038@stu.hit.edu.cn (D.Z.); gwang51@hit.edu.cn (G.W.); zzq@hitwh.edu.cn (Z.Z.)
* Correspondence: jlw@hit.edu.cn

Abstract: Reconfigurable intelligent surface (RIS) is emerging as a promising technology to achieve coverage enhancement. This paper develops a tractable analytical framework based on stochastic geometry for performance analysis of RIS-assisted millimeter wave networks. Based on the framework, a two-step cell association criterion is proposed, and the analytical expressions of the user association probability and the coverage probability in general scenarios are derived. In addition, the closed-form expressions of the two performance metrics in special cases are also provided. The simulation results verify the accuracy of the theoretically derived analytical expressions, and reveal the superiority of deploying RISs in millimeter wave networks and the effectiveness of the proposed cell association scheme to improve coverage. Furthermore, the effects of the RIS parameters and the BS density on coverage performance are also investigated.

Keywords: reconfigurable intelligent surface; millimeter wave; cell association; coverage probability; stochastic geometry

1. Introduction

Reconfigurable intelligent surfaces (RISs), consisting of elementary units called meta-atoms, can control wireless propagation, enhance link capacity, increase physical layer security, and extend network coverage by manipulating the phase and amplitude of reflected or refracted electromagnetic waves [1]. The emergence of RISs has changed the inherent paradigm of wireless communication system design, from passively adapting to the wireless environment to actively reshaping the electromagnetic environment [2]. RIS-assisted communications provide network planning engineers with new system design freedom, becoming one of the potential key technologies for sixth generation (6G) wireless mobile networks. At present, both academia and industry are striving to explore and evaluate the performance of RIS-assisted wireless communication networks by means of path loss models [3] and experimental measurements [4] of RIS-assisted links.

The RISs with controllable beams [5], low energy consumption [6], and flexible deployment [7] are regarded as a perfect patch for the blocking-sensitive millimeter wave networks. RIS-assisted millimeter wave networks are expected to provide mobile users with extremely high-speed, wide-area coverage, and high-quality communication services. In fact, RISs are suitable for various indoor and outdoor environments [8–10]. Ref. [8] established for the first time a universal indoor and outdoor channel model for RIS-assisted millimeter wave systems in the propagation environment with multiple random diffraction and scatterers. The model considers many physical characteristics and device characteristics, such as line-of-sight (LOS) probability, time delays, shadowing effects, actual gain of the RIS elements, and array response. The RIS channel simulator software package of [8] can be effectively applied to system-level simulations to evaluate the capacity, spectral efficiency, coverage performance and transmission rate of RIS-assisted systems by providing channel coefficients and electromagnetic environment parameters separately. It is well

known that human activities have a significant impact on indoor signal coverage. The authors of [9] comprehensively considered the occlusion effect of the human body and the probability distribution of the human position, and proposed an indoor RIS deployment strategy based on the human movement model. Furthermore, the proposed algorithm that minimizes the outage probability based on room geometry can calculate the corresponding RIS locations for single RIS deployments and multiple RISs collaborative deployments. The simulation results presented show that properly deployed RISs can significantly reduce the indoor millimeter wave communication outage probability. Given that both RISs and ultra-dense micro base stations (BSs) are used to enhance indoor millimeter wave wireless coverage quality, the authors of [10] explored which deployment option is more cost-effective. Through the joint analysis of coverage performance and deployment costs in a common indoor environment, the authors concluded that both pure active deployment and active-passive hybrid deployment can achieve the same network coverage. However, in order to meet coverage requirements with the lowest network cost, deploying an appropriate number of BSs is indispensable for RIS-assisted communication networks.

This paper mainly focuses on outdoor scenarios such as urban areas. Some outstanding researchers have studied the performance analysis of RIS-assisted outdoor millimeter wave networks, and this paper is an extension of their research results.

For blocking scenarios, i.e., assuming all direct links between BSs and users are non-line-of-sight (NLOS), Ref. [11] fully demonstrated the impacts of the RIS density on the area spectral efficiency improvement based on the conventional path loss model. The research results confirm that compared with traditional active networks, RIS-assisted networks effectively improve area spectral efficiency and achieve higher energy efficiency. In addition, the economic and maintenance costs of network deployment need to be considered in actual engineering applications, which results in the total density of network equipments being constrained. At this time, a compromise is required between the densities of RISs and BSs. However, the authors of [12] did not consider NLOS direct links, used random shape theory to model obstacles such as buildings, and derived the probability of the existence of LOS direct links. Then, the deployment strategies of RISs in different scenarios were studied. Research results show that for scenarios with dense obstacles, such as urban areas, deploying more small-scale RISs is a better choice to improve coverage, while large-scale RISs are more suitable for scenarios with sparse obstacles, such as rural areas. This paper considers a more realistic case where both LOS and NLOS coexist, adopting the LOS ball model in [13], and utilizes the path loss model for RIS-assisted transmission measured in [4].

Based on the analysis of signal-to-interference ratio (SIR), Ref. [14] verified the effectiveness of deploying RISs to improve the SIR coverage of millimeter wave networks from both theoretical analysis and simulation experiments. However, given that millimeter wave networks are non-interference limited [15], the impact of noise on system performance cannot be ignored. In addition, ref. [14] only considers Rayleigh fading in order to simplify the analysis. Refs. [11,12] directly ignore the impact of small-scale fading. In order to improve the universality of the research, this paper adopts a more generalized Nakagami-*m* fading.

Ref. [16] focused on RIS-assisted non-orthogonal multiple access networks, modeled linear RISs as the user-centered Poisson cluster processes, and derived analytical expressions for coverage and ergodic rate. Simulation results reveal that as the linear RIS length increases, there is an upper limit to system performance. Ref. [17] extended the carrier frequency in [16] to the millimeter wave band, modeled network elements as independent homogeneous Poisson point processes (HPPPs), and adopted an association criterion based on the maximum average received power. Furthermore, a statistical analysis of the distribution of signal-to-interference-plus-noise ratio (SINR) is performed. Simulation results show that for linear RISs, there is an optimal length to maximize the network coverage probability. This paper extends the one-dimensional linear model of RISs in [16,17] to the actual two-dimensional plane model and optimizes the cell association rules.

It can be seen from the above that the research results of this paper are more universal because the path loss model, fading model and RIS model used are more consistent with the

actual propagation environment. This paper provides a set of theoretical analysis results for coverage analysis of the RIS-assisted millimeter wave networks based on the stochastic geometric theory. The main contributions are summarized as follows:

- Cell association strategies directly affect user service quality. Different from the traditional one-step association strategies such as maximum average received power and nearest neighbor, we propose a two-step cell association criterion, where the first step is based on the minimum distance and the second step is based on the maximum average received power, which is equivalent to the minimum path loss.
- With the help of void probability, Slivnyak-Mecke theorem and probability generating functional in stochastic geometric theory, the tractable analytical expressions of user association probability and coverage probability for the general scenario are derived. Additionally, the asymptotic expression and closed-form upper bound of coverage probability are given for the ultra-dense and high-blocking scenarios, respectively.
- In fact, our paper provides a general numerical method for evaluating the coverage performance of RIS-assisted millimeter wave networks. Specifically, by substituting system parameters such as network element density and channel parameters into the formulas, we can directly obtain the value of the coverage probability without performing the system-level simulations such as Monte Carlo.

The remainder of this paper is organized as follows. The RIS-assisted millimeter wave system model is described in Section 2. In Section 3, the two-step cell association criterion is proposed. The analytical expressions of the coverage probability are provided in Section 4. Numerical and simulation results are presented in Section 5. Finally, Section 6 concludes this paper.

2. System Model

Consider a RIS-assisted millimeter wave network in which the distributions of BSs, RISs, and users are modeled as three independent HPPPs Φ_b, Φ_r, and Φ_u with densities λ_b, λ_r, and λ_u, respectively. The BS with no user connection is in idle mode, and otherwise in active mode [18]. The active BS distribution is also a HPPP Φ_B, whose density is expressed as:

$$\lambda_B = \lambda_b \left(1 - \left(1 + \frac{\lambda_u}{3.5\lambda_b} \right)^{-3.5} \right). \tag{1}$$

Assume a typical user under consideration is located at the origin. The typical user can receive signals directly from the BS or the RIS reflection; the former is called a direct link and the latter is called an RIS-assisted link. The communication links for the RIS-assisted millimeter wave network are shown in Figure 1. The LOS ball model suitable for dense network scenarios is adopted to distinguish whether the direct link is LOS or NLOS, then the path loss of the direct link can be expressed as:

$$L_d(x) = C_d x^{-a_L} \mathbb{I}(x \leq R_c) + C_d x^{-a_N} \mathbb{I}(x > R_c), \tag{2}$$

where $C_d = \left(\frac{\gamma}{4\pi} \right)^2$ is the intercept factor, γ is the wavelength, $\mathbb{I}(a)$ is the indicator function, x is the distance between the typical user and the BS, a_L and a_N are the LOS and NLOS path loss exponents, respectively, and R_c is the radius of LOS ball. Assume the typical user and the BS are both in the far field of the RIS, then the path loss of the RIS-assisted link is in the form of "distance products", denoted as:

$$L_r(y, z) = C_r(yz)^{-a_R}, \tag{3}$$

where $C_r = \frac{S\gamma^2}{64\pi^3}$ is the path loss intercept factor of RIS-assisted links [4], S is the RIS area, y is the distance between the RIS and the BS, z is the distance between the typical user and the RIS, and a_R is the path loss exponent of RIS-assisted links. It is generally assumed that $a_\kappa > 2$, where $\kappa = \{L, N, R\}$ [19]. Since the signal propagation of LOS direct

links and RIS-assisted links contains direct components, it is more universal to assume that they experience Nakagami-*m* fading. NLOS direct links are assumed to experience Rayleigh fading.
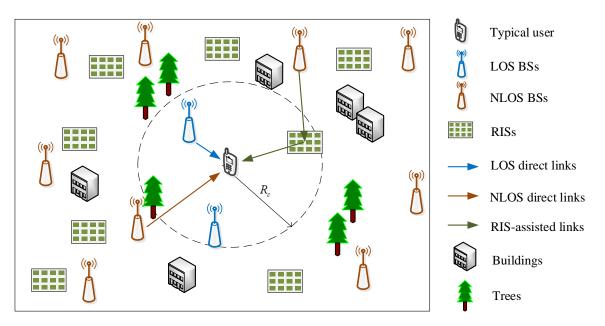

Figure 1. Communication links for reconfigurable intelligent surface (RIS)-assisted millimeter wave networks.

The transmit power of BSs is P_t. Antenna arrays at BSs perform directional beamforming. For tractability of analysis, the power pattern of antenna arrays is modeled as a simple sector model [13], in which the power gain of the main lobe with beamwidth θ is a constant M and the power gain of the side lobe with beamwidth $2\pi - \theta$ is a constant m. All users are equipped with omnidirectional single antenna. The serving BS adjusts the radiation direction to make the serving link obtains the maximum array gain M. The array gain of the *j*-th interfering link can be denoted as a discrete random variable D_j, whose value is M with probability $p_1 = \frac{\theta}{2\pi}$ and m with probability $p_2 = 1 - \frac{\theta}{2\pi}$.

3. Cell Association

Cell association criterion often directly affect network performance indicators such as user fairness, coverage, and transmission rate. In traditional active wireless networks, commonly used association strategies include nearest neighbor, maximum average received power, and maximum instantaneous SINR. Based on the above one-step association methods, we design a two-step cell association criterion for the RIS-assisted millimeter wave network, which is an active/passive hybrid wireless network. Specifically:

- First step: If the typical user can observe at least one LOS BS, connect to the nearest one.
- Second step: If there is no LOS BS observed, the typical user accesses the link with the smallest path loss, i.e., the typical user connects to the nearest NLOS BS or RIS, which reflects signals from the nearest BS.

Obviously, the derivation of user association probability is based on the statistical analysis of the nearest distance. The probability density functions (PDFs) of the distances from the typical user to its nearest NLOS BS and LOS BS are denoted as follows:

$$f_{x_n}^L(r) = 2\pi\lambda_b r \exp(-\pi\lambda_b r^2)\mathbb{I}(r \le R_c), \tag{4}$$

$$f_{x_n}^N(r) = 2\pi\lambda_b r \exp(-\pi\lambda_b r^2)\mathbb{I}(r > R_c). \tag{5}$$

The equivalent distance from the typical user to the nearest BS of the RIS-assisted link is defined as $w_n \overset{\Delta}{=} y_n z_n$, where y_n is the distance from the assist RIS to its nearest BS and z_n is the distance from the typical user to its nearest RIS. The PDFs of y_n and z_n are $f_{y_n}(r) = 2\pi\lambda_b r \exp(-\pi\lambda_b r^2)$ and $f_{z_n}(r) = 2\pi\lambda_r r \exp(-\pi\lambda_r r^2)$, respectively. The PDF of w_n is given by:

$$f_{w_n}^R(r) = 4\pi^2 r \lambda_b \lambda_r \mathcal{K}_0\left(2\pi r \sqrt{\lambda_b \lambda_r}\right), \tag{6}$$

where $\mathcal{K}_0(a)$ is the modified Bessel function of the third kind [20].

Next, the user association probability based on the two-step cell association criterion is given by Lemma 1.

Lemma 1. *The probability of the typical user associated with a LOS BS in the direct link is as follows:*

$$A_L = 1 - \exp\left(-\pi\lambda_b R_c^2\right). \tag{7}$$

The probability of the typical user associated with a NLOS BS in the direct link is:

$$A_N = \int_{\tilde{R}_c}^{\infty} \left[\exp\left(-\pi\lambda_b R_c^2\right) - \exp\left(-\pi\lambda_b \varphi^2(r)\right)\right] f_{w_n}^R(r) \mathrm{d}r, \tag{8}$$

where $\tilde{R}_c = \varphi^{-1}(R_c)$ with function $\varphi(x) = \left(4\pi S^{-1} x^{a_R}\right)^{\frac{1}{a_N}}$. The probability of the typical user connects to a RIS in the RIS-assisted link is $A_R = 1 - A_L - A_N$.

Proof. According to the void probability of HPPPs, (7) can be obtained. The proof of (8) is similar to Lemma 2 in [13], which is omitted here. □

For the case of no LOS direct links, i.e., $R_c = 0$, (8) can be written in the following closed form when $a_N = 2a_R$:

$$A_N = 1 - \frac{1}{\vartheta^2 - 1}\left[\frac{\vartheta}{\sqrt{\vartheta^2 - 1}} \ln\left(\vartheta + \sqrt{\vartheta^2 - 1}\right) - 1\right], \tag{9}$$

where $\vartheta = \frac{1}{2}\left(\frac{\lambda_b}{\lambda_r}\right)^{\frac{1}{2}}\left(\frac{4\pi}{S}\right)^{\frac{2}{a_N}}$.

Furthermore, the distribution of the distance from the typical user to its serving BS is given by Lemma 2.

Lemma 2. *Conditioning on that the typical user associated with a LOS BS in the direct link, the PDF of the distance to the serving BS is:*

$$\tilde{f}_{x_0}^L(r) = \frac{f_{x_n}^L(r)}{A_L}. \tag{10}$$

Given that the typical user connects to a NLOS BS, the PDF of the distance to the serving BS is:

$$\tilde{f}_{x_0}^N(r) = \frac{f_{x_n}^N(r)}{A_N} \int_{\varphi^{-1}(r)}^{\infty} f_{w_n}^R(t) \mathrm{d}t. \tag{11}$$

The PDF of the equivalent distance from the typical user to the serving BS in the RIS-assisted link is:

$$\tilde{f}_{w_0}^R(r) = \frac{f_{w_n}^R(r)}{A_R} \exp\left(-\pi\lambda_b R_c^2\right) \mathbb{I}(r \le \tilde{R}_c) + \frac{f_{w_n}^R(r)}{A_R} \exp\left(-\pi\lambda_b \varphi^2(r)\right) \mathbb{I}(r > \tilde{R}_c). \tag{12}$$

Proof. It can be proved by a method similar to Lemma 1. It is omitted here for brevity. □

4. Coverage Analysis

In this section, the SINR of the typical user is firstly analyzed, and then the analytical expression of the SINR coverage probability is given.

4.1. SINR Analysis

When the typical user connects to the LOS serving BS in the direct link, the performance is mainly limited by the interference from other LOS BSs, so the NLOS interference and the thermal noise are neglected. The SINR can be approximately expressed as:

$$\text{SINR}_L = \frac{M h_0^L x_0^{-a_L}}{I_L},\tag{13}$$

where $I_L = \sum_{j \in \Phi_B^L / b_0} h_j^L D_j x_j^{-a_L}$ is the LOS interference normalized by $P_t C_d$, Φ_B^L is the LOS BS set, the serving BS is denoted by b_0, the small-scale fading channel gain h_j^L follows a gamma distribution, expressed as $h_j^L \sim \text{Gamma}(g_L, 1/g_L)$, and shape parameter g_L is related to the physical propagation environment.

The SINR of the typical user associated with the NLOS BS in the direct link is as follows:

$$\text{SINR}_N = \frac{P_t M h_0^N C_d x_0^{-a_N}}{I_N + \sigma^2},\tag{14}$$

where $I_N = P_t C_d \sum_{j \in \Phi_B^N / b_0} h_j^N D_j x_j^{-a_N}$ is the interference from other BSs in the NLOS BS set Φ_B^N, h_j^N is the channel gain of NLOS direct links, following an exponential distribution with mean 1, and σ^2 is the power of additive white Gaussian noise.

When the typical user associates with the assist RIS, the SINR is given by:

$$\text{SINR}_R = \frac{P_t M h_0^R C_r w_0^{-a_R}}{I_N + I_R + \sigma^2},\tag{15}$$

where $I_R = \xi P_t C_r \sum_{i \in \tilde{\Phi}_B / b_0} h_i^R D_i (y_i z_n)^{-a_R}$ is the interference caused by the assist RIS reflecting the signals from interfering BSs. Similarly, as it is experiencing Nakagami-*m* fading, the small-scale fading channel gain is $h_j^R \sim \text{Gamma}(g_R, 1/g_R)$. It is assumed that only the reflected signals of the assist RIS point to the typical user, and other RISs do not interfere with the typical user. $\tilde{\Phi}_B$ is the set of interfering BSs located on the same side of the assist RIS as the serving BS. ξ is the interference factor, which is actually related to the incident angle difference between the interfering BS and the serving BS relative to the center point of the assist RIS. For tractability of analysis, the interference factor is assumed to be a constant.

4.2. Coverage Probability

The network coverage probability is defined as $P_c \triangleq \mathbb{P}(\text{SINR} \geq \tau)$, where τ is the SINR threshold. Based on Lemmas 1 and 2, and the total probability formula, P_c can be given by the following theorem.

Theorem 1. *The coverage probability P_c can be evaluated as:*

$$P_c = A_L P_c^L + A_N P_c^N + A_R P_c^R,\tag{16}$$

where $P_c^L \triangleq \mathbb{P}(\text{SINR}_L \geq \tau)$ is the coverage probability of the typical user associated with the LOS BS in the direct link, measured by:

$$P_c^L = \int_0^{R_c} \sum_{n=1}^{g_L} (-1)^{n+1} \binom{g_L}{n} \exp\left(-\pi \lambda_B r^2 \Psi_1(g_L, a_L, n\eta_L)\right)$$
$$\exp\left(\pi \lambda_B R_c^2 \Psi_1\left(g_L, a_L, n\eta_L r^{a_L} R_c^{-a_L}\right)\right) \tilde{f}_{x_0}^L(r) \mathrm{d}r,\tag{17}$$

where $\Psi_1(a,b,c) \triangleq \sum_{i=1}^{2} \beta_i \left[{}_2F_1(a, -\frac{2}{b}, 1 - \frac{2}{b}, -\frac{p_i \tau c}{a}) - 1 \right]$ *with* $\beta_1 = 1$, $\beta_2 = \frac{m}{M}$, ${}_2F_1(a,b;c;d)$ *is*

the Gauss hypergeometric function and $\eta_L = g_L(g_L!)^{-\frac{1}{g_L}}$; $P_c^N \triangleq \mathbb{P}(\text{SINR}_N \geq \tau)$ *is the coverage probability of the typical user connected to the NLOS BS in the direct link, computed as:*

$$P_c^N = \int_{R_c}^{\infty} \exp\left(-\delta r^2 \Psi_2(a_N, 1) \right) \exp(-v_N r^{a_N}) \tilde{f}_{x_0}^N(r) \mathrm{d}r, \tag{18}$$

where $\Psi_2(a,b) \triangleq \frac{b}{a-2} \sum_{i=1}^{2} \beta_i p_{i2} F_1\left(1, 1 - \frac{2}{a}; 2 - \frac{2}{a}; -\tau p_i b\right)$, $\delta = 2\pi \lambda_B \tau$, *and* $v_N = \frac{\sigma^2 \tau}{MP_t C_d}$; $P_c^R \triangleq$
$\mathbb{P}(\text{SINR}_R \geq \tau)$ *is the conditional coverage probability when the typical user access to the RIS-assisted link, given by:*

$$P_c^R = \int_0^{\infty} \int_0^{\infty} \sum_{n=1}^{g_R} (-1)^{n+1} \binom{g_R}{n} \exp\left(-\frac{\pi \lambda_B y^2}{2} \Psi_1(g_R, a_R, \xi n \eta_R) \right.$$
$$\left. -\delta \varphi^2(zy) \Psi_2(a_N, n\eta_R) - v_R(zy)^{a_R} \right) f(z,y) \mathrm{d}z \mathrm{d}y, \tag{19}$$

where $\eta_R = g_R(g_R!)^{-\frac{1}{g_R}}$, $v_R = \frac{\sigma^2 \tau n \eta_R}{MP_t C_r}$, *and* $f(z,y)$ *is denoted as:*

$$f(z,y) = \frac{f_{z_n}(z) f_{y_n}(y)}{A_R} \exp(-\pi \lambda_b R_c^2) \mathbb{I}(zy \leq \tilde{R}_c) + \frac{f_{z_n}(z) f_{y_n}(y)}{A_R} \exp(-\pi \lambda_b \varphi^2(zy)) \mathbb{I}(zy > \tilde{R}_c), \tag{20}$$

Proof. See Appendix A. □

For some special scenarios, the analytical expression of P_c can be simplified to a relatively simple form or even a closed form. The network coverage probability for the ultra-dense and high-blocking scenarios is given by Corollary 1 and Corollary 2, respectively.

Corollary 1. *For the ultra-dense case, the asymptotic expression of coverage probability is expressed as* $\tilde{P}_c^{UD} = A_L P_c^L$.

Proof. When $\lambda_b \to \infty$, $A_L \to 1$. Then, the asymptotic result can be obtained directly from (16). □

Corollary 2. *For the high-blocking case, the closed-form expression for a tight upper bound of coverage probability is given by:*

$$\bar{P}_c^{HB} = \sum_{n=1}^{g_R} (-1)^n \binom{g_R}{n} \frac{\alpha_1}{n} \exp\left(\frac{\alpha_2 \Psi_1(g_R, a_R, \xi n \eta_R) + \alpha_1}{n} \right) \text{Ei}\left(-\frac{\alpha_2 \Psi_1(g_R, a_R, \xi n \eta_R) + \alpha_1}{n} \right), \tag{21}$$

where $\alpha_1 = \frac{\pi^2 \lambda_b \lambda_r M P_t C_r}{\sigma^2 \tau \eta_R}$, $\alpha_2 = \frac{\pi^2 \lambda_B \lambda_r M P_t C_r}{2\sigma^2 \tau \eta_R}$, *and* $\text{Ei}(x)$ *is an exponential integral function.*

Proof. Users access the network through the RIS-assisted links because the signals of the direct links are severely attenuated in the high-blocking case, i.e., $A_R = 1$. We can reduce the exponential term $v_R(zy)^{a_R}$ in (19) to $v_R(zy)^2$, as follows:

$$\bar{P}_c^{HB} = \int_0^{\infty} \int_0^{\infty} \sum_{n=1}^{g_R} (-1)^{n+1} \binom{g_R}{n} \exp\left(-\frac{\pi \lambda_B y^2}{2} \Psi_1(g_R, a_R, \xi n \eta_R) \right.$$
$$\left. -\delta \varphi^2(zy) \Psi_2(a_N, n\eta_R) - v_R(zy)^2 \right) f(z,y) \mathrm{d}z \mathrm{d}y. \tag{22}$$

Then, with the help of Equation (3.352.4) and Equation (8.211.1) in [20], it is easy to obtain (21). □

5. Simulation Results

In this section, the proposed two-step cell association criterion, the analytical expression of coverage probability in general scenarios given by Theorem 1, and the closed-form expression of coverage probability in high-blocking scenarios given by Corollary 2 are verified by the Monte Carlo method where the main system parameters [13] shown in Table 1 are adopted if not mentioned otherwise and the RIS area S in square meters is set as $2000\gamma(M\lambda_r)^{-\frac{1}{2}}$. The number of simulations for each sampling point is 10^6. For each simulation, the network topology is generated within a disk with a radius of 5 km according to the stochastic geometric model described in Section 2, and the typical user is located in the center of the two dimensional region. Figure 2 visually presents the process of the Monte Carlo method. In addition, the effects of different system parameters on network coverage performance are shown in Figures 3–7, where the theoretical values obtained by the formulas are labeled "Formula", and the simulation results obtained by the Monte Carlo method are labeled "Simulation".

Figure 3 shows the coverage performance comparison of different cell association criteria and different network architectures. As it shows, when the SINR threshold is less than 12 dB, the two-step cell association criterion proposed in this paper achieves better coverage performance than the one-step cell association criterion in [17]; when the SINR threshold is greater than 12 dB, the performance of the two is almost the same. In addition, it can be observed that deploying RISs in millimeter wave networks can effectively improve the coverage probability because the RIS-assisted links have better channel conditions than NLOS links. Moreover, the theory results are almost the same as the Monte Carlo simulation results, verifying the accuracy of the analytical expressions in Theorem 1. Furthermore, it can also be observed that the coverage performance of the network decreases as the SINR threshold increases, which is obvious because the coverage probability is essentially the complementary cumulative distribution function of the SINR threshold.

Figure 4 shows the effects of the RIS area on the coverage performance. Note that according to the assumption of "far field" in Section 2, the RIS area needs to satisfy $S \leq 2000\gamma(M\lambda_r)^{-\frac{1}{2}}$ [4]. We can find the network coverage probability increases with the increase of RIS area due to the contribution of NLOS direct link and RIS-assisted link coverage performance improvement. However, there is no change in the coverage probability of LOS direct links for increasing the RIS area, since P_c^L is independent of S according to (17). Although using larger-area RISs can effectively improve network coverage, communication operators need to make a compromise between network performance and equipment cost during actual deployment. Ref. [2] conducts an in-depth study on the total deployment cost of active and passive hybrid networks under the premise of meeting performance requirements. Additionally, Figure 4 also reveals that the direct LOS links have extremely high coverage performance, which implies that stable transmission can be provided to users. This is because the LOS service BS is usually close to the user, resulting in relatively small signal loss.

A more complicated trend for the coverage performance is revealed in Figure 5. When the millimeter wave network is sparse, e.g., $\lambda_b < 10^2$ km^{-2}, the coverage probability quickly increases with λ_b, because the more BSs are deployed, the greater the probability of users accessing the LOS direct link. As for the dense scenario, e.g., 10^2 km$^{-2} \leq \lambda_b \leq 10^3$ km^{-2}, the coverage probability suffers rather slow growth and even decline in a certain BS density interval due to stronger interference experienced by users connected to the LOS direct link. When the network is ultra-dense, e.g., $\lambda_b > 10^3$ km^{-2}, the coverage probability is independent of the RIS density, and increases gradually with the increase of the BS density. In this scenario, the users are almost only associated with the LOS BSs, so the denser the BSs, the closer the users are to the serving BSs. Furthermore, the asymptotic results in Corollary 1 are the same as the theoretical results in Theorem 1, verifying the validity of the asymptotic expression for ultra-dense scenarios.
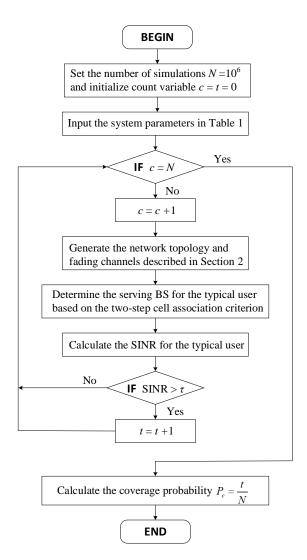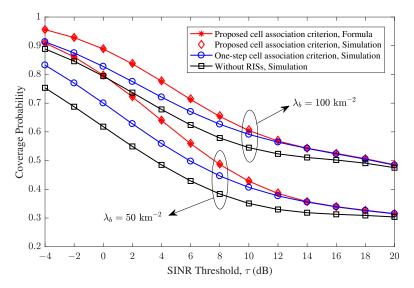
Figure 2. The process of the Monte Carlo method.
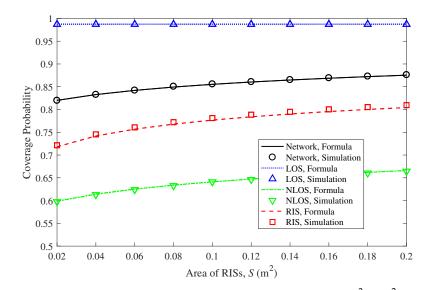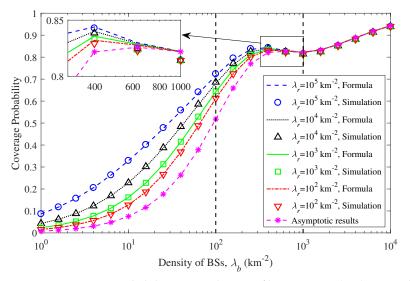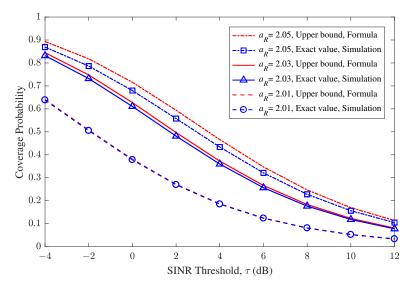

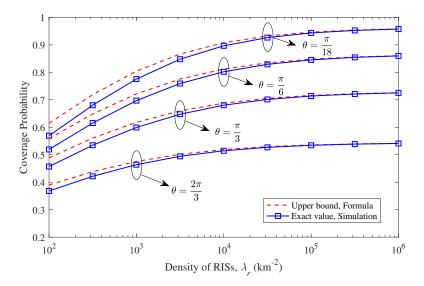**Figure 3.** Coverage probability versus signal-to-interference-plus-noise ratio (SINR) threshold.

Figure 4. Coverage probability versus area of RISs. $\lambda_r = 1 \times 10^3$ km^{-2}, $\tau = 0$ dB.

Figure 5. Coverage probability versus density of base stations (BSs). $\tau = 8$ dB.

Figure 6. Coverage probability for high-blocking cases with different τ and a_R.

Figure 7. Coverage probability for high-blocking cases with different λ_r and θ. $a_R = 2.03$, $\tau = 0$ dB.

Table 1. Parameter settings.

Parameter	Value
Carrier frequency	28 GHz
Bandwidth	100 MHz
BS transmit power, P_t	40 dBm
Noise power, σ^2	-94 dBm
Main lobe power gains of BS antenna arrays, M	10 dBi
Side lobe power gains of BS antenna arrays, m	-10 dBi
Main lobe beamwidth, θ	$\pi/3$
Path loss exponent of LOS direct links, a_L	2.1
Path loss exponent of NLOS direct links, a_N	4.2
Path loss exponent of RIS-assisted links, a_R	2.1
Shape parameter of Nakagami-m fading, g_L	3
Shape parameter of Nakagami-m fading, g_R	2
Radius of LOS ball, R_c	50 m
Interference factor, ξ	0.1
User density, λ_u	5×10^2 km^{-2}
BS density, λ_b	1×10^2 km^{-2}
RIS density, λ_r	2×10^3 km^{-2}

Figures 6 and 7 focus on high-blocking cases. As shown in Figure 6, the gap between the upper bound and the exact result gradually decreases as a_R tends to 2, which verifies the validity and applicability of the closed-form expression in Corollary 2. It can be seen from Figure 7 that narrowing the beamwidth of antennas effectively improve the coverage performance, because the narrower main lobe can reduce the interference from other BSs. Although the dense deployment of RISs also contributes to increasing the coverage probability, the efficiency of performance improvement is not high, and there is a coverage performance ceiling. Furthermore, as the RIS density increases, the gap between the upper bound and the exact value gradually decreases.

6. Conclusions

In this paper, the two-step cell association criterion was proposed for the RIS-assisted millimeter wave networks, and the tractable analytical expressions of the user association probability and the coverage probability were provided. The accuracy of the theoretical expressions was verified through Monte Carlo simulations. In addition, simulation results revealed that the proposed cell association criterion can achieve better coverage performance. Moreover, it is interesting to find that in sparse, dense, and ultra-dense scenarios, the coverage performance presents different trends with the increase of the density of BSs and RISs, which provides inspiration for system design and deployment. Furthermore, utilizing highly directional antennas is a more efficient method to improve coverage probability than densely deploying RISs.

Author Contributions: Conceptualization, G.W.; Methodology, D.Z.; Software, D.Z.; Formal analysis, D.Z.; Resources, J.W.; Writing—original draft, D.Z.; Writing—review & editing, G.W.; Project administration, J.W.; Funding acquisition, Z.Z. All authors have read and agreed to the published version of the manuscript.

Data Availability Statement: Data sharing is not available to this paper due to restrictions by funding organization.

Conflicts of Interest: The authors declare no conflict of interest.

Appendix A

Proof of Theorem 1. For brevity, only the proof of (19) is given, and the proofs of (17) and (18) follow a similar method:

$$
\begin{aligned}
P_c^R &= \mathbb{P}(\text{SINR}_R \geq \tau) \\
&\overset{(a)}{=} \int_0^\infty \mathbb{P}\left(h_0^R > \frac{(I_R + I_N + \sigma^2)\tau r^{a_R}}{P_t M C_r} \right) \tilde{f}_{w_0}^R(r)\,\mathrm{d}r \\
&\overset{(b)}{=} \int_0^\infty \int_0^\infty \mathbb{P}\left(h_0^R > \frac{(I_R + I_N + \sigma^2)\tau (zy)^{a_R}}{P_t M C_r} \right) f(z,y)\,\mathrm{d}z\,\mathrm{d}y,
\end{aligned}
\tag{A1}
$$

where (a) follows from (15) and the distribution of w_0, while (b) follows from $w_n = y_n z_n$.

$$
\begin{aligned}
\mathbb{P}\left(h_0^R > \frac{(I_R + I_N + \sigma^2)\tau (zy)^{a_R}}{P_t M C_r} \right) &\overset{(c)}{\approx} \mathbb{E}\left[1 - \left[1 - \exp\left(-\frac{\eta_R(I_R + I_N + \sigma^2)\tau(zy)^{a_R}}{P_t M C_r}\right) \right]^{g_R} \right] \\
&\overset{(d)}{=} \sum_{n=1}^{g_R} (-1)^{n+1} \binom{g_R}{n} \mathcal{L}_{I_R}(s_R)\mathcal{L}_{I_N}(s_R)\exp\left(-v_R(yz)^{a_R}\right),
\end{aligned}
\tag{A2}
$$

where $\mathcal{L}_I(s) = \mathbb{E}_I[\exp(-sI)]$ is the Laplace transform of I and $s_R = \frac{\tau n \eta_R (yz)^{a_R}}{P_t M C_r}$. Here, (c) follows from Lemma 6 in [13] and (d) is based on the Binomial theorem. Note that g_R is assumed to be an integer here, and the interpolation method in [2] can be used for the non-integer case.

Resorting to the derivation method similar to Proposition 1 in [21], we can obtain:

$$
\mathcal{L}_{I_R}(s_R) = \exp\left(-\frac{\pi \lambda_B y^2}{2} \Psi_1(g_R, a_R, \xi n \eta_R) \right).
\tag{A3}
$$

$$
\begin{aligned}
\mathcal{L}_{I_N}(s_R) &\stackrel{(e)}{=} \mathbb{E}_{\Phi_B^N}\left[\prod_{j \in \Phi_B^N / b_0} \frac{1}{1 + \tau n \eta_R \frac{C_d}{C_R} \frac{D_j}{M} (zy)^{a_R} x_j^{-a_N}} \right] \\
&\stackrel{(f)}{\geq} \exp\left(-2\pi\lambda_B \sum_{i=1}^{2} \beta_i \int_{\varphi(zy)}^{\infty} \frac{v}{1 + \frac{v^{a_N}}{4\pi S^{-1} \tau n \eta_R q_i (zy)^{a_R}}} \mathrm{d}v \right) \\
&\stackrel{(g)}{=} \exp\left(-\delta \varphi^2(zy) \Psi_2(a_N, n\eta_R)\right),
\end{aligned}
\tag{A4}
$$

where (e) directly follows from the distribution of h_j^N, (f) is based on the probability generating functional and reducing the lower limit of integral from R_c to $\varphi(zy)$ for the case $zy \leq \tilde{R}_c$, and (g) follows from Equation (3.194.2) in [20].

Then, substituting (A4), (A3), and (A2) into (A1), (19) is obtained. Finally, (16) is obtained based on the total probability formula. $\quad\square$

References

1. Zhao, D.; Wang, G.; Chen, G.; Jia, S. Coverage Analysis for Reconfigurable Intelligent Surface-Assisted Cellular Networks Over Nakagami-m Fading Channels. *IEEE Commun. Lett.* **2023**, *27*, 1035–1039. [CrossRef]
2. Lyu, J.; Zhang, R. Hybrid Active/Passive Wireless Network Aided by Intelligent Reflecting Surface: System Modeling and Performance Analysis. *IEEE Trans. Wirel. Commun.* **2021**, *20*, 7196–7212. [CrossRef]
3. Renzo, M.D.; Danufane, F.H.; Xi, X.; de Rosny, J.; Tretyakov, S. Analytical Modeling of the Path-Loss for Reconfigurable Intelligent Surfaces – Anomalous Mirror or Scatterer? In Proceedings of the 2020 IEEE 21st International Workshop on Signal Processing Advances in Wireless Communications (SPAWC), Atlanta, GA, USA, 26–29 May 2020 ; pp. 1–5.
4. Tang, W.; Chen, M.Z.; Chen, X.; Dai, J.Y.; Han, Y.; Renzo, M.D. Wireless Communications with Reconfigurable Intelligent Surface: Path Loss Modeling and Experimental Measurement. *IEEE Trans. Wirel. Commun.* **2021**, *20*, 421–439. [CrossRef]
5. Wu, Q.; Zhang, R. Intelligent Reflecting Surface Enhanced Wireless Network via Joint Active and Passive Beamforming. *IEEE Trans. Wirel. Commun.* **2019**, *18*, 5394–5409. [CrossRef]
6. Huang, C.; Zappone, A.; Alexandropoulos, G.C.; Debbah, M.; Yuen, C. Reconfigurable Intelligent Surfaces for Energy Efficiency in Wireless Communication. *IEEE Trans. Wirel. Commun.* **2021**, *18*, 4157–4170. [CrossRef]
7. Shafique, T.; Tabassum, H.; Hossain, E. Stochastic geometry analysis of IRS-assisted downlink cellular networks. *IEEE Trans. Commun.* **2022**, *70*, 1442–1456. [CrossRef]
8. Basar, E.; Yildirim, I.; Kilinc, F. Indoor and Outdoor Physical Channel Modeling and Efficient Positioning for Reconfigurable Intelligent Surfaces in mmWave Bands. *IEEE Trans. Commun.* **2021**, *69*, 8600–8611. [CrossRef]
9. Qin, H.; Liu, Z.; Yang, C. Indoor mm-Wave Coverage Enhancement: Reconfigurable Intelligent Surface Deployment Strategy Based on Human Mobility Model. *IEEE Commun. Lett.* **2022**, *26*, 2475–2479. [CrossRef]
10. Li, Z.; Hu, H.; Zhang, J.; Zhang, J. Enhancing indoor mmWave wireless coverage: Small-cell densification or reconfigurable intelligent surfaces deployment? *IEEE Wirel. Commun. Lett.* **2021**, *10*, 2547–2551. [CrossRef]
11. Zhu, Y.; Zheng, G.; Wong, K. Stochastic Geometry Analysis of Large Intelligent Surface-Assisted Millimeter Wave Networks. *IEEE J. Sel. Areas Commun.* **2020**, *38*, 1749–1762. [CrossRef]
12. Li, Z.; Hu, H.; Zhang, J.; Zhang, J. RIS-Assisted mmWave Networks With Random Blockages: Fewer Large RISs or More Small RISs? *IEEE Trans. Wirel. Commun.* **2023**, *22*, 986–1000. [CrossRef]
13. Bai, T.; Heath, R.W. Coverage and Rate Analysis for Millimeter-Wave Cellular Networks. *IEEE Trans. Wirel. Commun.* **2015**, *14*, 1100–1114. [CrossRef]
14. Nemati, M.; Park, J.; Choi, J. RIS-Assisted Coverage Enhancement in Millimeter-Wave Cellular Networks. *IEEE Access* **2020**, *8*, 188171–188185. [CrossRef]
15. Rappaport, T.S.; Sun, S.; Mayzus, R.; Zhao, H.; Azar, Y.; Wang, K.; Wong, G.N.; Schulz, J.K.; Samimi, M.; Gutierrez, F . Millimeter wave mobile communications for 5G cellular: It will work! *IEEE Access* **2013**, *1*, 335–349. [CrossRef]
16. Zhang, C.; Yi, W.; Liu, Y.; Yang, K.; Ding, Z. Reconfigurable Intelligent Surfaces Aided Multi-Cell NOMA Networks: A Stochastic Geometry Model. *IEEE Trans. Commun.* **2022**, *70*, 951–966. [CrossRef]
17. Xie, Z.; Yi, W.; Wu, X.; Liu, Y.; Nallanathan, A. Modeling and Coverage Analysis for RIS-aided NOMA Transmissions in Heterogeneous. *arXiv preprint* **2021**, arXiv:2104.13182.
18. Lee, S.; Huang, K. Coverage and economy of cellular networks with many base stations. *IEEE Commun. Lett.* **2012**, *16*, 1038–1040. [CrossRef]
19. Andrews, J.G.; Baccelli, F.; Ganti, R.K. A Tractable Approach to Coverage and Rate in Cellular Networks. *IEEE Trans. Commun.* **2011**, *59*, 3122–3134. [CrossRef]

20. Gradshteyn, I.M.; Ryzhik, I.M. *Table of Integrals, Series, and Products*, 7th ed.; Academic Press: Cambridge, MA, USA, 2007.
21. Liu, D.; Yang, C. Caching Policy Toward Maximal Success Probability and Area Spectral Efficiency of Cache-Enabled HetNets. *IEEE Trans. Commun.* **2017**, *65*, 2699–2714. [CrossRef]